Time-variant rule-based reliability of corroded structures by Monte Carlo simulation

IOP Conf. Series: Materials Science and Engineering **700** (2019) 012036 doi:10.1088/1757-899X/700/1/012036

Time-variant rule-based reliability of corroded structures by Monte Carlo simulation

K M Neumann[1,*], B Leira[2], O T Vårdal[3] and S Ehlers[4]

[1] Wood, Structural & Marine Technology department, Kokstadflaten 35, Bergen, Norway
[2] NTNU, Institute of Marine Technology, Otto Nielsens veg 10, Trondheim, Norway
[3] AHPA,Sildaberget 22a, 5171 Loddefjord, Norway
[4] TUHH, Institute for Ship Structural Design and Analysis, Am Schwarzenberg Campus 4 C, Hamburg, Germany

*Corresponding author: karoline.neumann@woodplc.com

Abstract. General widespread corrosion is of increasing concern for structural reliability of ageing marine structures, particularly for semi-submersible pontoons. Conditional failure rate, also termed hazard function is sought to describe the increasing maintenance required with age. Literature is reviewed connecting corrosion degradation to hazard rate, either through a time degrading limit state function, or statistical data for time to failure. Here, a rule based failure definition is applied based on corrosion tolerance levels, together with a linear corrosion degradation model to make a time variant limit state function. Monte Carlo simulation is applied based on statistical models for the basic variables including importance sampling, to obtain the time to failure distribution from which the hazard curve is deduced. A more realistic hazard function is also produced, requiring average of 3 simulations to exceed the tolerance in order to fail. It is seen that this approach delays the increase of the hazard curve, at the expense of higher failure rates.

1. Introduction

General widespread corrosion is a threat to structural reliability of ageing floating marine offshore structures. Particularly, the ballast tanks in pontoons of old semi-submersibles are of concern because they are not available for inspection or repair when in operation, and the environment is susceptible to corrosion. Additionally ballast tanks are closed spaces which have to be gas freed, and entering is associated with hazard. Sometimes scaffolding is necessary for close inspection, which is imposing increased coast and risk. A search on the ship-info.com database gives 42 results for drilling rigs, and 12 results for accommodation rigs built prior to 1999. These are 54 semi-submersibles which currently have exceeded their initial design period which is typically 20 years. Corrosion in ballast tanks may be kept at bay for long periods with coating and sacrificial anodes, despite this, general widespread corrosion is common in ageing pontoons. Considering that the coating system after several years gradually breaks down, and the corrosion from this time starts to progress at slightly various rates, more and more corrosion will exceed our tolerance limits. The objective is to describe the increasing failure rate using the hazard curve. Ageing can be described by the hazard function, often termed bath-tub curve, and is according to Ersdal poorly utilized or forgotten [1]. A report produced for the Norwegian Petroleum Safety Authority (PSA) states that additional information is needed on deterioration and its

modeling to determine the form of the bath-tub curve, and the start of wear out phase [2]. It will be analysed if the shape of the hazard curve will follow the usual bath-tub shape with a probabilistic linear corrosion model. The hazard curve for a corroding structure will be obtained by simulating the parameters coating breakdown, corrosion rate and original thickness by Monte Carlo simulation and calculating notional probability of failure through the limit state function, in Section 3. During operation of a unit observations can be gathered and used to update the distributions of the input parameters to increase the relevance of the prediction. The resulting hazard curve is presented in Section 4. First, a review is performed relating hazard function to corrosion through the application of time-variant structural reliability methods.

2. Structural reliability methods applied on corrosion

Garbatov and Guedes Soares analysed a dataset of corrosion on tankers and bulk carriers subject to permissible tolerance levels to obtain time to failure, T. Reliability $L = P(T \leq t)$ was presented as a function of time, and used to decide between different maintenance strategies [3]. Barone and Frangopol considers a bridge described by a limit state including corrosion degradation, and performs bi-objective optimization between total maintenance cost and several key performance indicators (kpi), one of them being the hazard function, h(t) [4]. It is found that hazard function gives similar results as availability as kpi, but hazard function is computationally cheaper [4]. Akpan considers general corrosion degradation of the ultimate hull girder bending moment capacity as limit state, and presents failure probability considering varying corrosion distributions and parameters [5] [6]. The reliability or probability of survival, L, is calculated through the hazard function, h(t), according to Equation 1. The deduction of this formula is presented in Rausand and Høyland's book page 19 [7]. Ellingwood and Mori developed the model of ageing structural reliability of concrete components to assess probability of failure with time in nuclear plants [8]. The hazard function was presented for various degradation models and parameters. Moan and Ayala-Uraga incorporates the effect of corrosion on the fatigue limit state of components of a ship. The hazard rate and the cumulative probability of failure is presented, and it is concluded that the hazard rate is a better measure, and that not considering corrosion effects on fatigue is non-conservative [9].

$$L(t) = exp(-\int_0^t h(t)dt) \tag{1}$$

3. Method

The limit state is reached when crossing from the safe to the failure region, in other words when load effect S, exceeds resistance R. The difference between the resistance and the load effect is termed the safety margin, or just margin M, and describes the limit state function. An illustration of the time dependent limit state with constant limit S and time variant remaining thickness R(t) is seen in Figure 1. Cumulative probability of failure at time t, F(t) is defined by the probability that the limit state function or margin, M is less or equal to zero, or the probability that a failure will occur any time prior to t, according to Equation 2. The former is typically used when a theoretical model is available such that M can be computed, the latter is used when statistical data of time to failure, T of a number of components is available. The reliability is in any case L(t)=1-F(t). Here we will use a model to define M, according to Equation 3, and simulate time to failure using Monte Carlo simulation of the involved variables as will be explained in Section 3.2. Resistance, R is here remaining thickness, which is original thickness t_{orig} minus corrosion diminution, d(t), which will be elaborated in Section 3.1. Load effect S is a rule based discrete minimum allowable remaining thickness based on DNVGL-CG-0172 Thickness Diminution for Mobile Offshore Units [10]. For secondary category area for column-based units minimum 85% of original thickness remaining is required. This gives

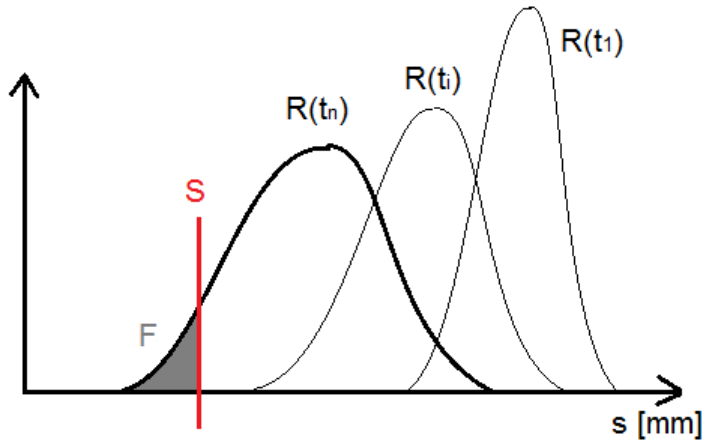

Figure 1. Illustration of limit state where S is load effect and R is resistance

a deterministic value of the acceptable limit of S =10.2mm for a 12mm thickness structure considered here. Different categories of structures such as primary or special would yield another percentage requirement, and other thicknesses would result in other discrete mm failure limits. For simplicity, only a 12 mm secondary structures is considered here. A secondary structure gives a higher allowance than primary or special members, so the results will give an optimistic scenario relative to other categories. The definition of failure here is corrosion diminution exceedance of this rule based limit, similar to Garbatov's failure definition based on tolerance levels, rather than the physical load effect [3]. Unlike ships where global failure modes of the ship hull beam can be defined, every failure mode of every component have to be separately addressed for the semi-submersible. To avoid this, the rules based limit is more practicable and more useful from a maintenance perspective. The notional cumulative failure probability, F for the given input is calculated by counting numbers of failures divided by total number of simulations in the Monte Carlo method as explained in Section 3.2. By derivation of F(t), the corresponding failure density f(t) can be calculated, termed the instantaneous failure rate in the interval $[-0.5\Delta t < t < 0.5\Delta t]$, which can be computed numerically for discrete years according to Equation 4. The conditional failure rate in the same interval, given that no failure has occurred prior to t is termed hazard function, and defined as in Equation 5, see eg. [7] [9].Another illustration of time-variant thickness and deterministic tolerance level is seen in Figure 2.

$$F(t) = P(M(t) \leq 0) = P(T \leq t) \tag{2}$$

$$M = R(t) - S = t_{orig} - d(t) - S \tag{3}$$

$$f(t) = F(t) - F(t-1) \tag{4}$$

$$h(t) = \frac{f(t)}{1 - F(t)} \tag{5}$$

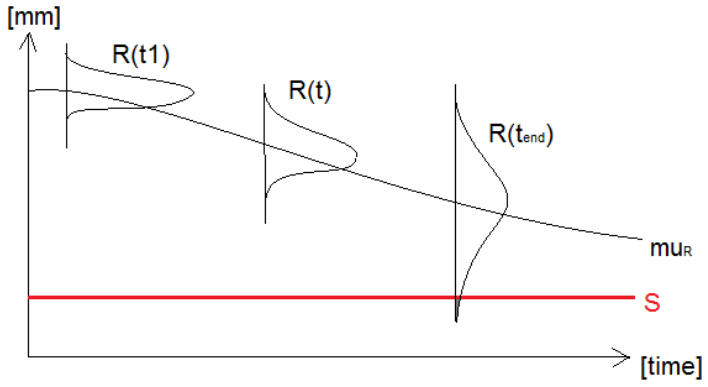

Figure 2. Illustration of time variant reliability in the case of corrosion degradation of resistance and constant rule based limit S.

3.1. Corrosion modeling and parameters

A simplification of Paik's model in Equation 6 is used to model the corrosion degradation with time t in years, with exponent C2 = 1 so that it presents a linear model, and transition time $T_t = 0$, so that corrosion is assumed to suddenly start progressing. This is in line with Melchers and Southwells suggestions and C1 equals corrosion rate [11] [12]. The applied model for thickness diminution d(t) in mm, is presented in Equation 7. Here, the original thickness t_{orig} is represented by the variable X1 in mm, the time of coating breakdown (Tc) by the variable X3 in years, and the corrosion rate c_{rate} by the variable X2 [mm/y]. Then Equation 3 can be written in the form of Equation 8. The applied target distributions for each variable is presented in Table 1. Original thickness is also modeled, since measurements of old corroded structures can show a substantial amount of 'increasing' thicknesses compared to nominal, such as the sunken MV Chester, or more than half of the readings in a campaign reported by Luque [13][14]. The mean is taken as the mid of upper and lower tolerances of class A steel of 12 mm according to EN10029, and the standard deviation of X1 is 1/3 of the tolerance span from the mean to each side at 1.7/2 mm (lower=-0.5, upper=+1.2). Then the tolerance is interpreted as 99.7 percentile which equals 3*standard deviation. Corrosion rate, X2, is also assumed to follow a truncated normal distribution.

The values are based on measurements of more than 1000 locations on uncoated ballast tanks of an old semi-submersible, measured at the same location with 5 years interval. The mean value may seem low at first glance, compared to literature on ships' ballast tanks, reporting from 0.043 mm/y to 0.1 mm/y [15] [13]. However, ballast tanks in ships are more often emptied and filled compared to semi-submersibles which maintain the same ballast for long periods on location to keep submerged. Hence smaller corrosion rates may be expected due to a less corrosive environment with less mixing of water and air. Also the applied standard deviation for X2 at 0.1 may seem high, but is taken the same as Yamamoto, although Wang reports values as low as 0.038 [16] [17]. Since the corrosion rate was deduced from measurements that were taken in an old structure, the high standard deviation is due to a highly uneven surface. Different distributions of coating breakdown time is suggested in the literature, such as a lognormal [18], [11] and normal [19], [20]. Here a truncated normal distribution will be applied for X3 with parameters as seen in Table 1 where mean and standard deviation are loosely inspired by [20]. Each parameter is simulated using Monte Carlo (MC) simulation, with importance sampling (IS) for variables X2, and X3.

$$d_{paik}(t) = C_1 * (t - T_c - T_t)^{C_2} \tag{6}$$

$$d(t) = (t - T_c) * c_{rate} = (t - X3) * X2 \tag{7}$$

$$M(t) = X1 - (t - X3) * X2 - S \tag{8}$$

Table 1. Target distributions and parameters of variables

Variable	Distribution	Mean	Standard deviation
X1 (original thickness)	Normal	12.35 mm	0.85/3
X2 (corrosion rate)	Normal truncated at 0	0.01 mm/y	0.1
X3 (coating breakdown)	Normal truncated at 0	9.5 y	3

3.2. Monte Carlo simulations

Brute Monte Carlo simulation involves choosing (pseudo) random values between 0 and 1 on a uniform distribution, and finding the corresponding value of each variable x by use of the inverse cumulative distribution function of the variable, as illustrated in Figure 3. The discrete combination of x values are used to calculate the margin. Each discrete calculation of M is checked for failure or no failure. After many simulations, probability of failure can be calculated by dividing number of failures by total number of simulations. This approach will be applied here, and is illustrated for 3 variables X1, X2 and X3 and constant S in Figure 1.

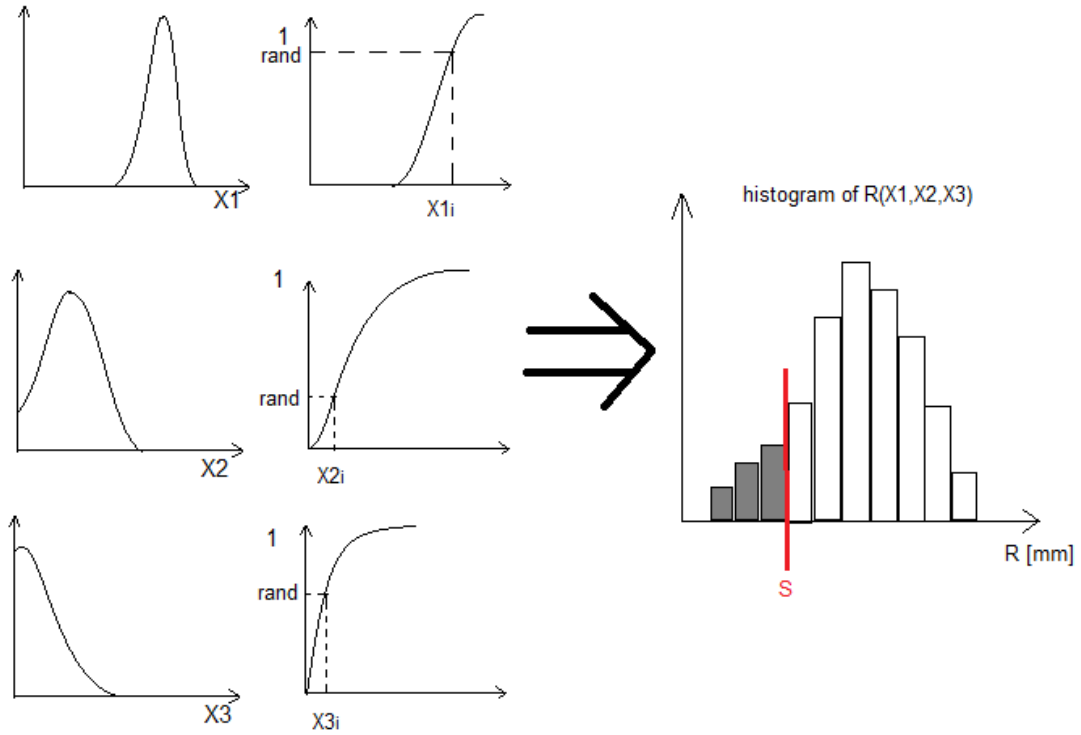

Figure 3. Illustration of Monte Carlo simulation of M with 3 variables and discrete S

3.2.1. Importance sampling Importance sampling is performed to get a better estimate of the small probabilities of failure. This is particular in the cases where X3 is small and X2 is large, or X3 is large and X2 small. Since these combinations are so unlikely, a usual Monte Carlo sampling from X2 and X3 target distributions would give us very little failed combinations in these cases. The solution is to sample from a different proposal distribution that will pick combinations both resulting in failure and safe combinations on a more equal basis, as will be seen later in Figure 8. When computing the probability of failure, F, the fact that the target distributions (which are the realistic ones) is not used has to be compensated for by a weighing factor p/q as in Equation 9, where p is the target distribution and q is the proposed distribution for weighting. Here, the proposed distributions for X2 and X3 are the same as for the target distributions, but with standard deviation 5 times as high. Figure 4 illustrated this for a few simulations for variable X2, showing a much more uniform distribution that will give more weight to higher corrosion rates than the target distribution.

$$F = \frac{1}{N}\sum_{n=1}^{N}(M \leq 0) \cdot \frac{p(x)}{q(x)} \tag{9}$$

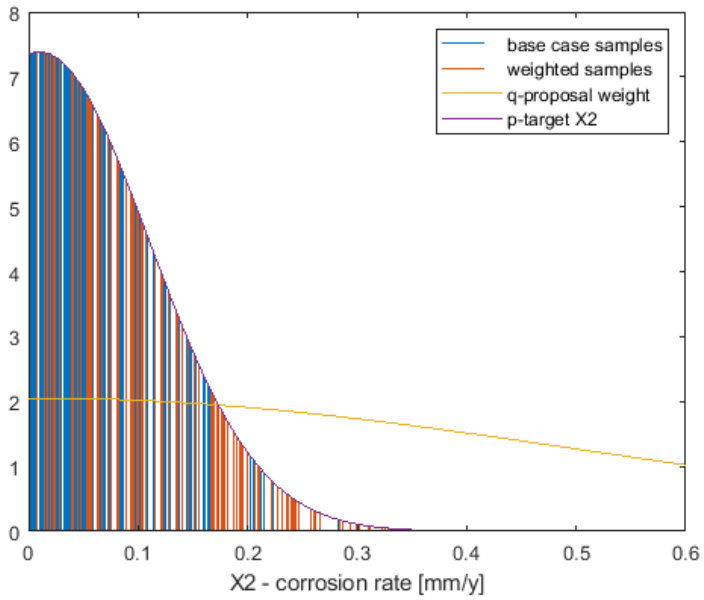

Figure 4. Importance sampling of variable X2, where q is the proposal distribution which IS is tanken from, and p is the target distribution of X2 given in Table 1.

3.3. Pseudo-code

A flow chart for the matlab script to calculate probability of failure is presented in Figure 5. First the the discrete values, S, original thickness, n iterations and y total years as well as counters i and t are initialized. Also the distribution for the variables X1, X2 and X3 is assigned, together with corresponding parameters according to Table 1. Using a pseudo-random algorithm, an array of n random realizations are generated for each variable, assuming they are all statistically independent. Then diminution d, remaining thickness R and margin M are calculated according to Equations 7 and 3 for the first set of simulated variables. If the margin

is less than 0, it is considered a failure and will be counted as $fail = fail + 1$, before it will increment to next simulated variable and perform the same check until M is calculated for all simulated combinations of variables. Then probability of failure for the given year is calculated as a relative sum of failures $F(t) = fail/n$. The probability of failure is cumulative with years and corresponds to the cumulative distribution function of the instantaneous failure density, calculated by Equation 4, hence the hazard function can be calculated according to Equation 5. Then the procedure is to repeat this for each year, since corrosion diminution d is time variant. The counter for failures, 'fail' will be set to zero as t iterates to the next year.When this is performed for all years, the loops end, and relevant figures are plotted.

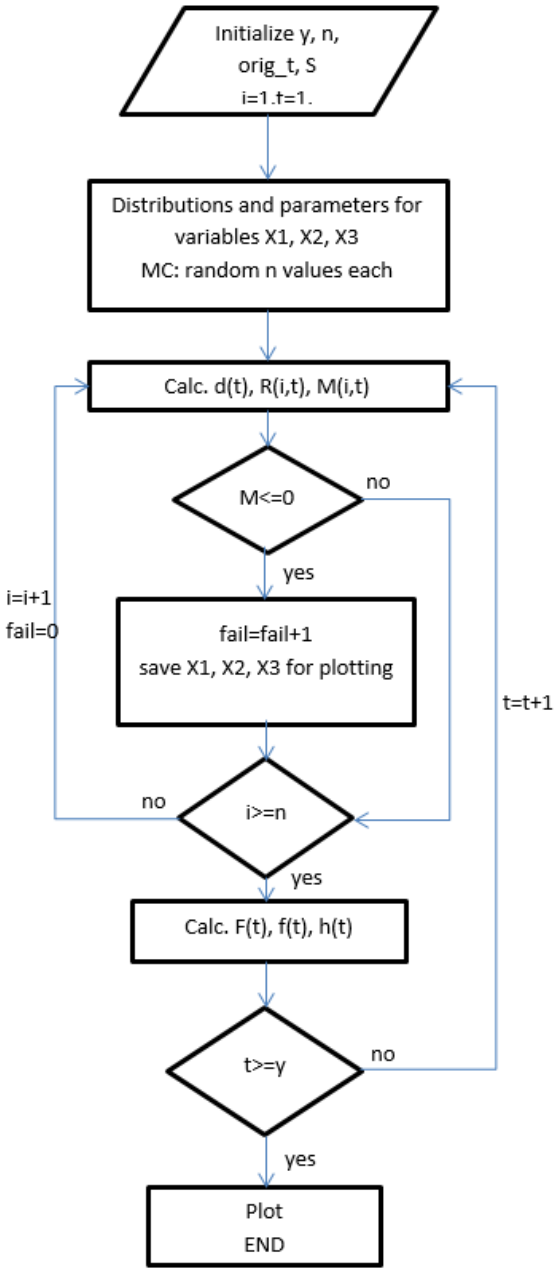

Figure 5. Flow chart for computation of F in matlab script

4. Results and discussion

4.1. Distribution of diminution and remaining thickness

An impression of the corrosion progression and distribution according to the simulation is presented in Figure 6, where the histogram is normalized to an area of 1. It can be seen that both the mean and the variance increases with time. The graph is truncated in the vertical direction to get a better look at the flatter distributions. The 5 years distribution is much higher near zero, explaining the seemingly small area. In Figure 7, simulated remaining thickness R is plotted for a selection of years. Again it is normalised, and cut in the vertical axis, as well as in the lower end of the horizontal axis. At year 40, the probability to measure thicknesses exceeding the original nominal thickness, 12 mm, $P(d = 0 \mid t = 40) = 0.09$. Similarly there is a 13% chance at 30 years and a 75% chance at 10 years of measuring values greater than the nominal thickness, with the values applied in this simulation.

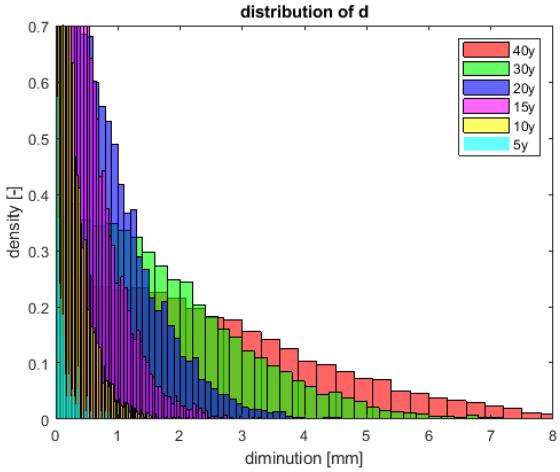

Figure 6. Simulated corrosion diminution d, for a selection of years.

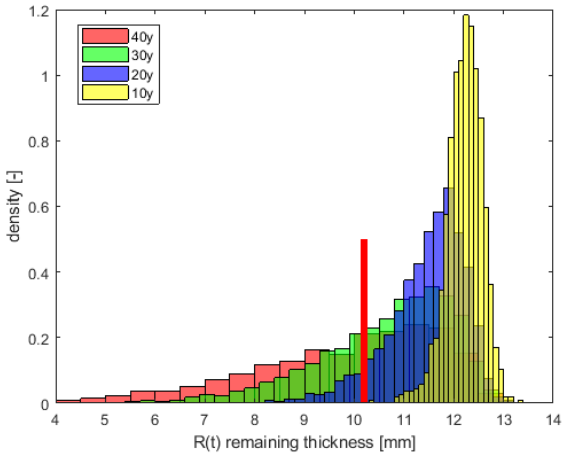

Figure 7. Simulated R, remaining thickness, and minimum allowable remaining thickness S is shown as a red line.

4.2. Failure regions

The failure planes in the physical plane for a diminution corresponding to 10,20,30 and 40 years is seen in Figure 8, together with 3000 samples simulated using importance sampling. IS samples from the proposed distributions are distributed more evenly between the failure regions and fall on both sides of the planes. Samples from the target distribution would have concentrated on the mean, giving few points close to the edges. Upper right corner represents safe side, and opposite side of the planes, towards left lower corner, represents failure region. As the years pass, the failure planes move closer and closer towards upper right corner, increasing the probability of failure. It can be seen that the planes lean slightly, in X1 axis, showing initially high original thicknesses survive slightly longer. In Figure 9 the failure planes are plotted in 2D, seen from above. Here safe region is towards lower right corner, and fail towards upper left. The leaning of the planes in X3 axis is then transformed to thickness of the lines representing variations in original thickness. It can be seen that for high corrosion rate, failure will occur almost immediately after coating breakdown Tc, while for low corrosion rates, failure is dominated more and more by time to coating breakdown as years pass. For the 10 year plane, et least the area spanned by 8 years coating breakdown or more, and less than 0.1 mm/y corrosion rate is safe. When 40 years have passed, at least all combinations with corrosion rate larger than 0.25 mm/y and coating breakdown less than 29 years have failed.

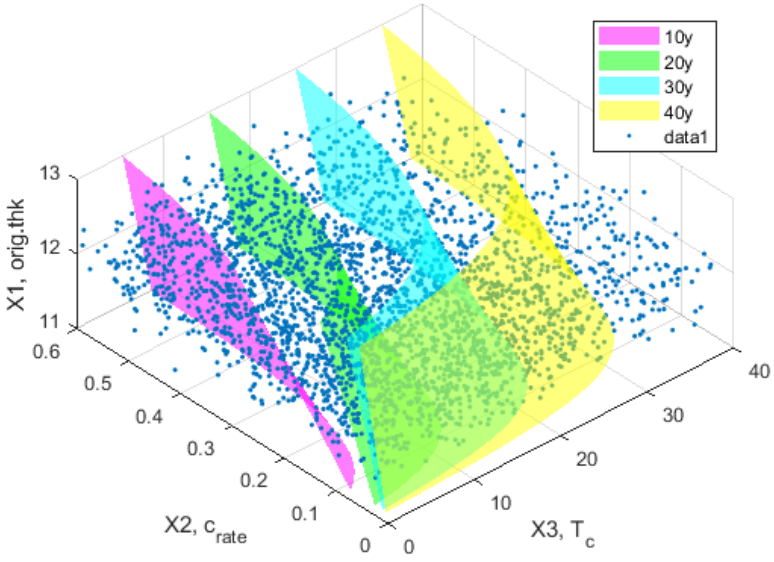

Figure 8. Failure planes in physical space together with IS samples

4.3. Time-variant probability of failure

The simulated time-variant cumulative probability of failure is shown in Figure 10, using 3 million simulations. This graphs shows that the failures are slow in the beginning, only starting after 10 years. Then the number of failures increases rapidly, reaching an inflection point before 25 years. This inflection point corresponds to the peak of the instantaneous unconditional failure rate, f(t), which is plotted in Figure 11 together with the instantaneous conditional failure rate, h(t), called hazard function. While f(t) δt is number of failures in interval δt divided by total simulations, h(t) δt is number of failures in the same interval, divided by number of simulations

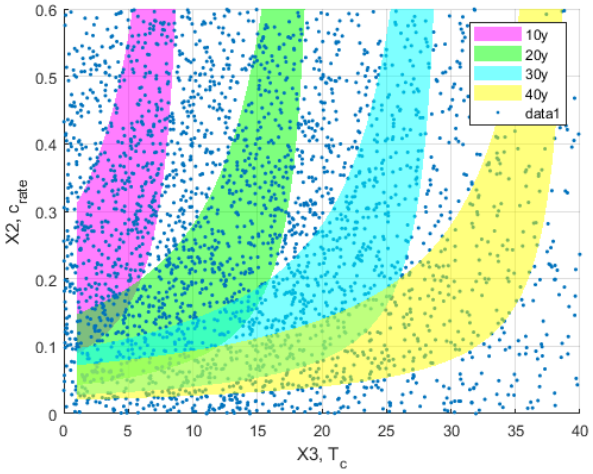

Figure 9. Failure planes in 2D in physical space together with IS samples

that have not failed yet. Failure as referred to until now represent too low individual thicknesses.

For a more useful case, the failure criterion can be defined when average of three thicknesses are below the rule-based limit, S, hereafter termed the average of three definition of failure. The three measurements are spaced equally in a component of size in the range of meters and are considered independent. According to Melchers, independent samples of corroded thickness are obtained already after 5 mm spacing, while a more recent study finds no correlation over 40 mm spacing [21] [22]. In practice the average of three approach may be the case in the yard. Measuring three thicknesses at a plate, stiffener or any other component reduces the uncertainty. A component failing according to this definition requires remediation or repair. This average of three definition is used when producing Figure 12. This Figure is shifted in relation to Figure 11, meaning that in practice, although individual measurements start to exceed the regulatory limit around 10 years, this is still allowed, because single measurements does not represent the component as a whole. Components regulatory failures are not starting until age of 15. Here only original components are accounted for, without regard of what happens to the failed components. It is seen that the average of three approach delays the onset of the hazard curve, at the expense of higher failure rates.

4.4. Errors and convergence

In Figure 13 the simulated probability of failure F is plotted as a function of number of simulations for selected years. For low amount of simulations, the graph is fluctuating. When reaching $3 * 10^6$ simulations the values have stabilised. Importance sampling contributes to this. The variance in the probability of failure is presented in Table 2 and is considered sufficiently low.

5. Discussion

Some may be surprised that the presented hazard curve do not have the shape of a bath-tub. This is due to the input, where all the corrosion is modeled according to the same distributions. In further work, multiple distributions for X1, X2 and X3 could be considered, representing different structures and corrosive areas. Then a few areas may be very prone to corrosion, which will all fail very early causing an early bump. The increasing wear-out part of the curve is

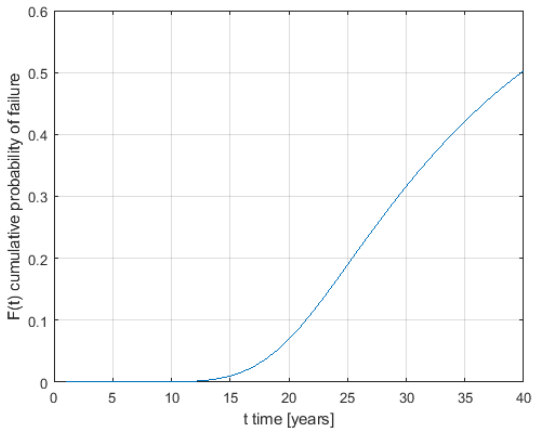

Figure 10. Time variant probability of failure, F, in [0 t].

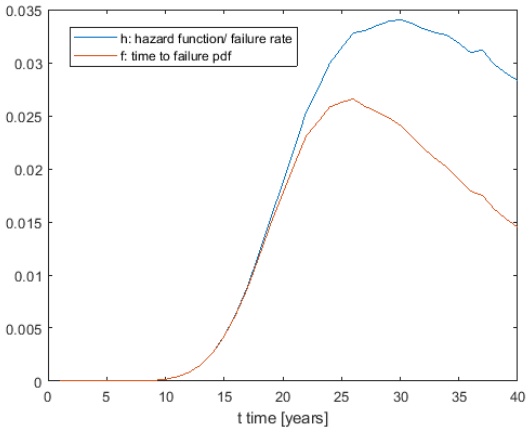

Figure 11. Instantanous failure density function f(t), and conditional failure rate h(t).

Table 2. Variance and probability of failure for selected years at 3 million simulations

Years	F	Variance
5	$1.4 * 10^-6$	$4.7 * 10^-13$
10	$9 * 10^-4$	$3.1 * 10^-10$
15	0.0221	$7.4 * 10^-9$
20	0.1184	$3.9 * 10^-8$
30	0.4006	$1.1 * 10^-7$
40	0.5749	$1.3 * 10^-7$

expected, but yet another surprise is the subsequent decreasing part. Does it mean that once the bump is passed, the maintenance can be decreased? Overall, most likely no. The presented hazard curve represents only the failure frequency of the original remaining parts that have not failed yet, not taking into account what happened to all those failures in the past. In reality,

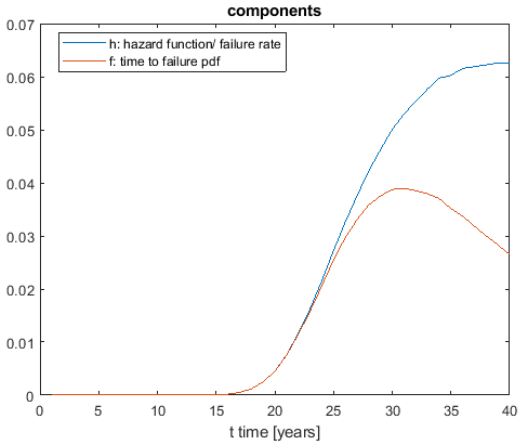

Figure 12. Instantanous failure density function f(t), and conditional failure rate h(t) for components failures, applying average of three failure definition.

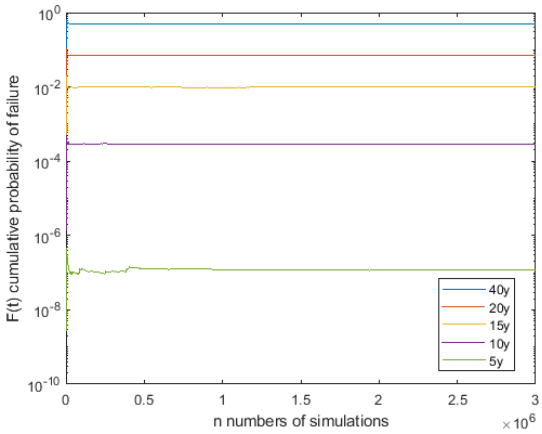

Figure 13. Probability of failure as a function of simulations for selected years

the failed parts were fixed, and by the time the presented hazard curve decreases, then the parts that were fixed early on probably starts failing again. These failures are not accounted for. However the required maintenance of the remaining non-failed parts past the bump may be decreased. Consider an example where, after 40 years, a plate in a protected void space may be shifted for the first time which is accounted for in the hazard rate, while in the same year several plates in the trim tank are replaced for the second time, which is not counted the second time in the hazard rate. Then again, if the previously failed components are fixed forever to never fail again, the hazard rate would decrease. In further studies the effect of combining various structural components, failure tolerances and corrosive environments could be investigated, in addition to how different corrosion models than the linear approach would affect the hazard curve.

6. Conclusion

The hazard rate is presented for a corroding semi-submersible pontoon applying Monte Carlo simulation to model the time variant probability of failure. It is seen that the average of

three approach delays the onset of the increase of the hazard curve, at the expense of higher failure rates. The hazard curve may be a tool to help management decisions regarding future maintenance regimes or scrapping. It may also be used as a performance indicator for comparing assets, or optimizing cost. It can also be concluded that the expected number of measurements higher than nominal thickness is low for units exceeding their design life according to this model. It is proposed that further work may include the implication on hazard curve by using different corrosion models, including spatio-temporal descriptions. Also, various distributions could be applied for the variables X1, X2, X3 to represent different structures and corrosive environments.

References

[1] Ersdal G, Hörnlund E and Spilde H 2011 *Proc. of the ASME 2011 30th Int. Conf. on Ocean, Offshore and Arctic Engineering* January 2011 pp 517–522 ISBN 9780791844359
[2] Galbraith D and Sharp J 2007 Recommendations for Design Life Extension Regulations Tech. rep. PSA Stavanger
[3] Garbatov Y and Guedes Soares C 2010 *Maintenance planning for the decks of bulk carriers and tankers* (Taylor & Francis)
[4] Barone G and Frangopol D M 2014 *Struct. Saf.* **48** 40–50
[5] Akpan U O, Koko T S, Ayyub B and Dunbar T E 2003 *Nav. Eng. J.* **115** 37–48
[6] Akpan U O, Koko T S, Ayyub B and Dunbar T E 2002 *Mar. Struct* **15** 211–231 ISSN 09518339
[7] Rausand M and Høyland A *System reliability theory: models, statistical methods, and applications* 2nd ed (Hoboken, New Jersey: John Wiley & Sons) ISBN 3175723993
[8] Ellingwood B R and Mori Y 1993 *Nucl. Eng. Des* **142** 155–166 ISSN 00295493
[9] Moan T and Ayala-Uraga E 2008 *Reliab. Eng. Syst. Saf.* **93** 433–446 ISSN 09518320
[10] DNV-GL 2015 DNVGL-CG-0172 Thickness Diminution for Mobile Offshore Units
[11] Paik J K, Lee J M, Park Y I, Hwang J S and Kim C W 2003 *Mar. Struct* **16** 567–600 ISSN 09518339
[12] Melchers R E 2013 *Corros Sci* **68** 186–194 ISSN 0010938X
[13] Stambaugh K A and Knecht J C 1991 SSC-348 Corrosion experience data requirements Tech. rep. Ship Structural Committee Washington DC
[14] Luque J, Hamann R and Straub D 2014 *Proc. of the ASME 2014 33rd Int. Conf. on Ocean, Offshore and Arctic Engineering*
[15] Paik J K, Lee J M, Hwang J S and Park Y I 2003 *Mar. Technol.* **40** 201–217
[16] Yamamoto N and Ikegami K 1998 *J. Offshore Mech. Arct. Eng.* **120** 121–128
[17] Wang G, Spencer J and Sun H 2005 *J. Offshore Mech. Arct. Eng.* **127** 167–174 ISSN 08927219
[18] Guo J, Wang G, Ivanov L and Perakis A N 2008 *Mar. Struct* **21** 402–419 ISSN 09518339
[19] Qin S and Cui W 2003 *Mar. Struct.* **16** 15–34 ISSN 09518339
[20] Melchers R E and Jiang X 2006 *Ships Offshore Struc* **1** 61–70 ISSN 1744-5302
[21] Melchers R, Ahammed M, Jeffrey R and Simundic G 2010 *Mar. Struct.* **23** 274–287 ISSN 09518339
[22] Neumann K M and Ehlers S 2019 *Proc. of the ASME 2019 38th Int. Conf. on Ocean, Offshore and Arctic Engineering* (Glasgow: ASME)